



Importance of self-shielding in mass measurements using γ -ray spectroscopy

JESSE D NORRIS¹ and SHIKHA PRASAD^{2,*}

¹Lawrence Livermore National Laboratory, Livermore, CA 94550, USA

²Department of Nuclear Engineering, Texas A&M University, College Station, TX 77843, USA

*Corresponding author. E-mail: shikhap@tamu.edu

MS received 16 September 2019; accepted 24 April 2020; published online 20 July 2020

Abstract. Due to the exponential attenuation of photons in materials, thick samples will attenuate a large portion of photons. This is a source of error in methods such as neutron activation analysis, which use gamma spectroscopy to characterise a radioactive source. A method is developed to quantify the magnitude of self-shielding with the help of MCNP6. Then the mass of an unknown sample is determined by comparing the known sample mass and the photopeak counts of the unknown and the known samples following activation. The inclusion of self-shielding effects is shown to make this comparative mass analysis measurement technique more accurate. Accounting for the self-shielding effects allows the true source, instead of the shielded source, to be resolved by correcting for the photons that are attenuated as they try to escape the sample and reach the detector. The γ -ray measurements were made using several samples of varying shapes.

Keywords. Self-shielding; self-attenuation; neutron activation analysis; comparative mass analysis; gamma spectroscopy.

PACS Nos 12.60.Jv; 12.10.Dm; 98.80.Cq; 11.30.Hv

1. Introduction

Gamma spectroscopy measures the photon energy spectrum emitted from a radioactive source. This measurement relies on a sufficient number of photons reaching the detector and contributing to the photopeak. However, as photons are born within a source they are exponentially attenuated and scattered within the source structure [1]. This process is referred to as self-absorption, self-attenuation, or gamma self-shielding [2–4]. Here it will be called self-shielding, to emphasise that the source is shielding itself from the detector.

A problem arises when measuring thick sources because many photons are attenuated or scattered before reaching the detector. These photons do not contribute to the photopeak and represent lost information about the source. In order to resolve the characteristics of the source, these photons must be accounted for. This can be done by estimating the magnitude of self-shielding based on the size, composition, and orientation of the source and the detector used to measure it [3,4]. In this work, we shall focus on the size and shape of the sample being irradiated.

Self-shielding is always present to some extent. In some cases, the loss of information can be neglected. However, self-shielding effects should be quantified in large samples to estimate uncertainty any time the quantitative information is being measured from the source. Self-shielding analysis has been applied to nuclear waste management and decommissioning [2], naturally occurring radioactive material in the oil and gas industry [5] and prompt γ -ray neutron activation analysis [6]. In those contexts, the focus has been on defining self-shielding as a function of photon energy for specific materials, determining analytic solutions for simple geometries and applying Monte Carlo simulations to estimate the mass attenuation coefficient of a sample.

This work will focus on an extension of neutron activation analysis (NAA), measuring the mass of an unknown sample by comparing it to a known sample [7], referred to as comparative mass analysis (CMA). There has been success in this area under the assumptions that the source is thin in terms of gamma attenuation and similar geometries are compared [7,8]. This work will apply to heterogeneous geometries and thick objects by taking self-shielding of γ -rays in aluminum into

account. A Monte Carlo simulation using MCNP6 will be employed to quantify the effects of self-shielding for specific experiments and it is show that taking self-shielding into account more accurately measures the unknown mass.

2. Theory

When exposed to neutron radiation, normally stable isotopes may undergo radiative capture and become radioactive. If the newly created radioisotope emits a measurable photon flux during its decay, subsequent gamma spectroscopy can be used to determine the characteristics of the source. By relating the measured photopeaks and activities of the isotopes within the sample, NAA can qualitatively or quantitatively determine the composition of the source. In a similar fashion, CMA has been used to accurately determine the mass of unknown samples using neutron irradiation or natural decay of radioactive elements [7]. This is done using the relationship

$$m_2 = \frac{C_2 m_1 e^{\lambda_2 \delta_2} \int_0^E \sigma_1(E) \phi(E) dE \alpha_1 \epsilon_{D_1} \epsilon_{G_1} \Gamma_1}{C_1 e^{\lambda_1 \delta_1} \int_0^E \sigma_2(E) \phi(E) dE \alpha_2 \epsilon_{D_2} \epsilon_{G_2} \Gamma_2},$$

$$\alpha_1 = (1 - e^{-\lambda_1 t_{\text{irr}_1}})(1 - e^{-\lambda_1 \Delta_1}),$$

$$\alpha_2 = (1 - e^{-\lambda_2 t_{\text{irr}_2}})(1 - e^{-\lambda_2 \Delta_2}), \quad (1)$$

where m is the mass, C is the counts in the photopeak of interest, λ is the decay constant, $\int \sigma(E) \phi(E) dE$, or the product of the neutron capture microscopic cross-section and the neutron scalar flux integrated over all neutron energies, is the production rate of the radioisotope of interest per target nuclide, t_{irr} is the irradiation time, δ is the time between the end of irradiation and beginning of measurement, Δ is the measurement time, ϵ_D is the intrinsic detector efficiency, ϵ_G is the geometric efficiency of the detector and the sample, Γ is the branching ratio and the subscripts 1 and 2 denote the known and unknown samples, respectively [7,8]. In cases such as those presented here with a single element and the same irradiating source for all cases, the term $\int \sigma(E) \phi(E) dE$ is the same in the numerator and denominator of eq. (1) and cancels out.

Equation (1) has been successfully applied to samples of thin uniform shapes and single element homogeneous compositions, where self-shielding is assumed to be negligible [7]. The dependence on the production rate, the intrinsic detector efficiency and the branching ratio is removed by comparing the photopeak of a single radioisotope between samples, simplifying eq. (1) to

$$m_2 = \frac{C_2 m_1 e^{\lambda_2 \delta_2} (1 - e^{-\lambda_1 t_{\text{irr}_1}})(1 - e^{-\lambda_1 \Delta_1}) \epsilon_{G_1}}{C_1 e^{\lambda_1 \delta_1} (1 - e^{-\lambda_2 t_{\text{irr}_2}})(1 - e^{-\lambda_2 \Delta_2}) \epsilon_{G_2}}. \quad (2)$$

Any analysis using gamma spectroscopy will suffer if there is an appreciable amount of self-shielding by the source. When this is the case, self-shielding can no longer be ignored. To account for the magnitude of attenuated photons, another term f_{SS} is included,

$$m_2 = \frac{f_{SS_1} C_2 m_1 e^{\lambda_2 \delta_2} (1 - e^{-\lambda_1 t_{\text{irr}_1}})(1 - e^{-\lambda_1 \Delta_1}) \epsilon_{D_1} \epsilon_{G_1}}{f_{SS_2} C_1 e^{\lambda_1 \delta_1} (1 - e^{-\lambda_2 t_{\text{irr}_2}})(1 - e^{-\lambda_2 \Delta_2}) \epsilon_{D_2} \epsilon_{G_2}}, \quad (3)$$

where f_{SS_1} is the self-shielding factor of the known mass and f_{SS_2} is the self-shielding factor of the unknown mass.

This self-shielding factor is determined by characterising the escape probability of a photon from the sample, similar to that of [3,4,9]. The self-shielding factor can be determined by averaging this photon escape probability throughout the detector crystal volume. Furthermore, the photon must contribute to the photopeak. Therefore, the self-shielding factor for any photon that could contribute to the photopeak by interacting within the detector crystal can be defined as

$$f_{SS} = \frac{N_e}{N_b}, \quad (4)$$

where N_e is number of photons exiting the sample without interaction and N_b is number of photons born within the sample. Here, $f_{SS} \leq 1$ and approaches unity as attenuation from the sample becomes negligible.

Equation (4) is therefore the ratio between the measurable case, where photon interaction occurs within the sample, and the idealised case, where no photon interaction occurs within the sample and the maximum number of photons contributing to the photopeak reach the detector crystal. This factor is not directly measured through experimentation, but a Monte Carlo simulation is utilised to model the sample and the detector, with a photon source homogeneously distributed throughout the sample. Then, the photon flux at the energy of the photopeak with and without the sample is tallied within the volume of the detector crystal, such that

$$f_{SS} = \frac{\text{photon track lengths with the sample}}{\text{photon track lengths without the sample}}. \quad (5)$$

This is done by voiding the sample volume while maintaining the source, in order to model the photon flux in the detector crystal without any attenuation.



Figure 1. Aluminum cylindrical bowl set-up at IIT-Kanpur.

3. Method

Four measurements were performed to determine the effect of this self-shielding factor on CMA. Different sample geometries were used to change the magnitude of self-shielding. The measurements were performed at the Radiation Detection Laboratory, Indian Institute of Technology-Kanpur. The source was a ^{239}Pu -Be neutron Howitzer manufactured in November 1967 with an alpha-neutron activity of 5Ci [10]. The source has a measured thermal neutron flux of $1.1 \times 10^5 \text{ cm}^{-2} \text{ s}^{-1}$ [7]. Each irradiation lasted approximately 15 min, or seven half-lives of the radioactive nuclide formed (i.e. ^{28}Al , with $T_{1/2} = 2.2$ min), to reach saturation. The sample was then moved to a separate location for measurement. This resulted in a time delay of nearly 2 min, or about one half-life, between the end of irradiation and start of the measurement.

The measurements were performed using a high-purity germanium detector (HPGe). Figure 1 shows an example of the HPGe measuring a sample. The samples were placed close to the face of the detector in order to improve the counting statistics by increasing the solid angle of the sample in relation to the detector. This was necessary due to the relatively small neutron capture cross-section of ^{27}Al and the low thermal neutron flux of the ^{239}Pu -Be neutron Howitzer. The measurement was then modelled in MCNP6 to quantify the self-shielding factor and geometric efficiency. The process was repeated under similar conditions for the known comparator. Finally, eqs (2) and (3) were used to determine the mass of the unknown sample with and without accounting for self-shielding.

3.1 Samples

Three samples were used in the four experiments. All the samples were assumed to be natural aluminum with a density of 2.7 g/cm^3 , consisting entirely of ^{27}Al . Aluminum does not have perfect characteristics for neutron activation, and has a thermal neutron capture cross-section of only 0.231 b [11]. However, the 2.24 min half-life of its daughter, ^{28}Al , and 100% emission probability of the 1.779 MeV photon with every decay help to complete measurements with acceptable counting statistics in a short amount of time [12].

The three sample geometries tested are: cylindrical bowl, rectangular cuboid comprising five uniformly sized slabs and a hollow sphere. The cylindrical bowl was fabricated from an aluminum ingot different from the sphere and slabs. Figure 2 shows the diagram of the three geometries. Table 1 shows the dimensions of the samples in terms of the mean free path (MFP) of a 1.779-MeV photon in natural aluminum (8.08 cm) [13].

3.2 Simulations

The general radiation transport code MCNP6 was chosen to determine the self-shielding factor due to its extensive verification and validation [14]. Careful measurements were recorded during the experiments to accurately model the position and orientation of the samples and the detector. The sample was modelled with a 1.779 MeV photon source homogeneously distributed throughout its volume.

A Canberra GC2018 Coaxial HPGe detector was used for the measurements. This detector has a cylindrical crystal of 61.9 mm diameter and 32.8 mm thickness with a window distance of 4.84 mm. Figure 3 shows the

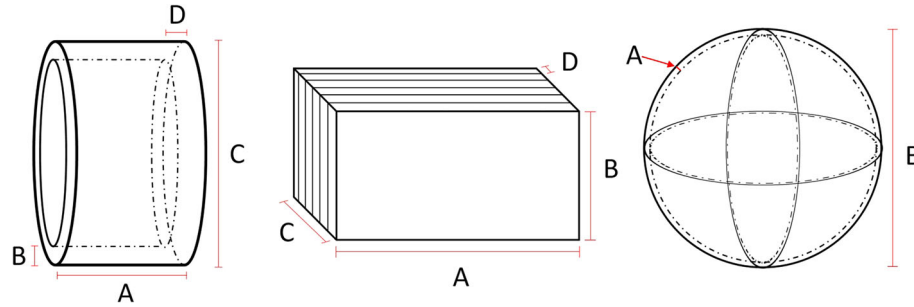


Figure 2. Samples used for mass comparison. Left to right: cylindrical bowl, rectangular cuboid and hollow sphere.

Table 1. Sample dimensions in figure 2.

Sample	A	B	C	D
<i>Dimension (cm)</i>				
Cylindrical bowl	5.5	1.25	11.5	1.5
Rectangular cuboid	9.9	4.95	4.95	0.95
Hollow sphere	0.4	10.95	–	–
<i>Fraction of MFP</i>				
Cylindrical bowl	0.681	0.155	1.42	0.186
Rectangular cuboid	1.23	0.613	0.613	0.118
Hollow sphere	0.05	1.36	–	–

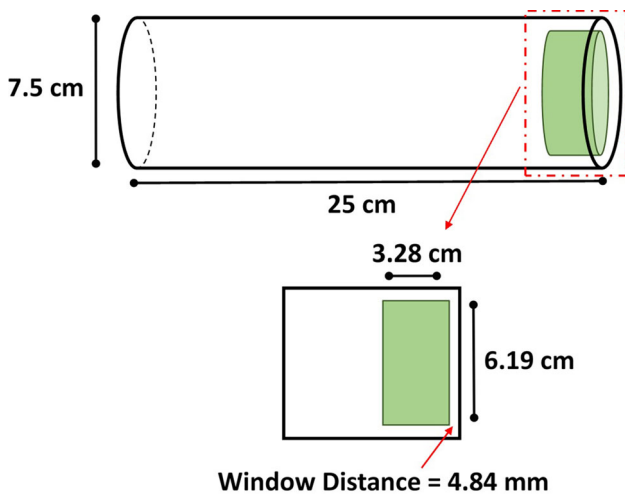


Figure 3. HPGe detector dimensions: the shaded portion corresponds to the HPGe detector crystal and the larger cylinder corresponds to the outer aluminum housing, seen in figure 1.

diagram of the crystal size and dimensions within its aluminum casing. The detector was modelled with a volume, equivalent in size and position, to its crystal within MCNP6.

Two simulations are needed to determine the self-shielding factor. First with the sample present, resulting in self-attenuation of the photons. Then again with the sample voided, resulting in no self-attenuation of the

photons. Both simulations use the cell-averaged photon flux tally (F4 tally in MCNP) within the detector crystal volume. Taking the ratio of these two fluxes yields the self-shielding factor (f_{SS}) for the experiment, as defined in eq. (5). Included in these simulations is a surface current tally (F1 tally in MCNP) for photons of the photopeak energy. This tally is used to determine the geometric efficiency (ϵ_G) of the sample with respect to the detector.

This combination of F4 tally and F1 tally to determine the self-shielding factor and geometric efficiency, respectively, was chosen for its simplicity. A pulse height tally (F8 tally in MCNP) could also measure the energy deposition within the detector crystal volume while taking the geometric efficiency into account.

Fundamentally, the simulations need to determine the fraction of photons that are removed due to self-attenuation by the sample. All other interactions (i.e. incidence and interaction within the detector crystal), with respect to the unattenuated photons leaving the sample, will be consistent between both simulations and cancel out in the ratio of eq. (5). This allows everything but the sample, when present, to be voided. Any interaction of a photon at energy E after the photon escapes the sample is independent of the presence of the sample.

In addition, another simulation was performed to determine the geometric efficiency of the sample using a surface current tally with respect to the detector volume.

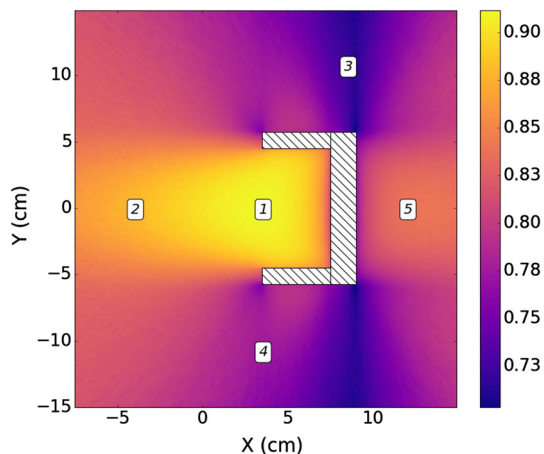


Figure 4. Spatial variation of the self-shielding factor.

Table 2. Self-shielding factors at the five positions in figure 4.

Point	1	2	3	4	5
f_{SS}	0.91	0.88	0.72	0.78	0.84

Table 3. Summary of experiments.

Case	Comparator	Unknown
1	Three slabs	Single slab
2	Three slabs	Five slabs
3	Five slabs	Cylindrical bowl
4	Five slabs	Hollow sphere

4. Results and analysis

An example of the spatial variation in the self-shielding factor of the cylindrical aluminum bowl was calculated using the MCNP6 cell-average photon flux mesh tally, shown in figure 4. The figure shows a cross-section directly through the centre of the bowl. The self-shielding factors at the five positions noted in this figure are included in table 2.

The self-shielding factor around the bowl can vary by as much as 20% just by rotating the sample to 90°. Further, the factor could vary significantly throughout the detector crystal. By utilising the cell-averaged flux tally within the crystal volume, this potentially large spatial variation is accounted for.

The four experiments are summarised in table 3. The first and second use a varying number of slabs with the rectangular cuboid in figure 2. The third and fourth experiments use the full rectangular cuboid as the comparator to measure the cylindrical bowl and the hollow sphere.

For cases 1 and 2, the slab samples were placed axially symmetric and 5 cm away from the detector. These three measurements were preformed sequentially. Table 4 summarises the values from cases 1 and 2. For cases 3 and 4, the samples were again placed axially symmetric and 3.5 cm away from the detector. However, the hollow sphere had to be placed 3 cm away from the detector to prevent it from rolling around. Table 5 summarises the values from cases 3 and 4.

All the values in tables 4 and 5 were calculated by using a cell-averaged flux tally for f_{SS} or a current tally for ϵ_G on the HPGGe crystal volume. Their uncertainty represents the statistical uncertainty from the Monte Carlo method, but not the potential systematic uncertainties in the model. The uncertainty in the counts, by far the largest contribution to statistical uncertainty, is from the stochastic process of decay.

Figures 5 and 6 present the unknown mass approximation using eqs (2) and (3) to show that the addition of the self-shielding factor more accurately predicts the unknown mass. Table 6 summarises the measured mass and associate uncertainty with and without taking self-shielding into account. Cases 1 and 4 capture the true mass within one standard deviation after applying the self-shielding factor. Case 2 captures the true mass within two standard deviations. Case 3, using the cylindrical aluminum bowl, is greater than three standard deviations away after applying the self-shielding factor, potential reasons are discussed next. For all cases, the systematic error in mass approximation after applying the self-shielding factor improves and decreased by a factor 2 or more. This is because the attenuated gamma rays or the lost information is accounted for in the calculation. This can also be verified by the columns labelled $\Delta_{m_{SS}}\%$ and $\Delta_m\%$ giving the percent deviation from the actual measured masses given in the second column for each case. For case 1, the best improvement is seen where the deviation reduces from -7.992 to just 0.498% . For case 3, a much lower improvement is seen where the deviation from the actual mass is reduced from 34.17 to 17.53% .

Largest deviation seen in case 3 could be due to a few reasons. First, the cylindrical bowl was made from a different ingot than the comparator (in all other cases the sample in question and the comparator were made from the same ingot). Thus, the assumption that the density and percent abundance of Al in the sample are the same in the numerator and denominator of eq. (3) and will cancel is not accurate for case 3, that of the cylindrical bowl. Second, a prominent manganese photopeak at 846 keV is visible in the energy spectrum of the cylindrical bowl, emanating from the first observation and validating the dissimilarities in the compositions of cylindrical bowl and the comparator, which have not

Table 4. Self-shielding factors and geometric efficiencies for all samples used in the experiments.

	One slab		Three slabs		Five slabs	
	Value	σ	Value	σ	Value	σ
Mass (g)	127.5	–	402.3	–	683.2	–
Counts	636	27	1317	38	1733	45
f_{SS}	0.943	1.05×10^{-3}	0.840	1.43×10^{-3}	0.769	1.74×10^{-3}
ϵ_G	0.0448	5.66×10^{-5}	0.0366	5.11×10^{-5}	0.0309	4.69×10^{-5}

Table 5. Self-shielding factors and geometric efficiencies for all samples used in the experiments.

	Five slabs		Cylindrical bowl		Hollow sphere	
	Value	σ	Value	σ	Value	σ
Mass (g)	683.2	–	888.3	–	376	–
Counts	1925	48	2214	51	765	34
f_{SS}	0.775	1.01×10^{-3}	0.885	1.04×10^{-3}	0.893	2.47×10^{-3}
ϵ_G	0.0430	1.93×10^{-4}	0.0289	1.74×10^{-4}	0.0285	2.68×10^{-4}

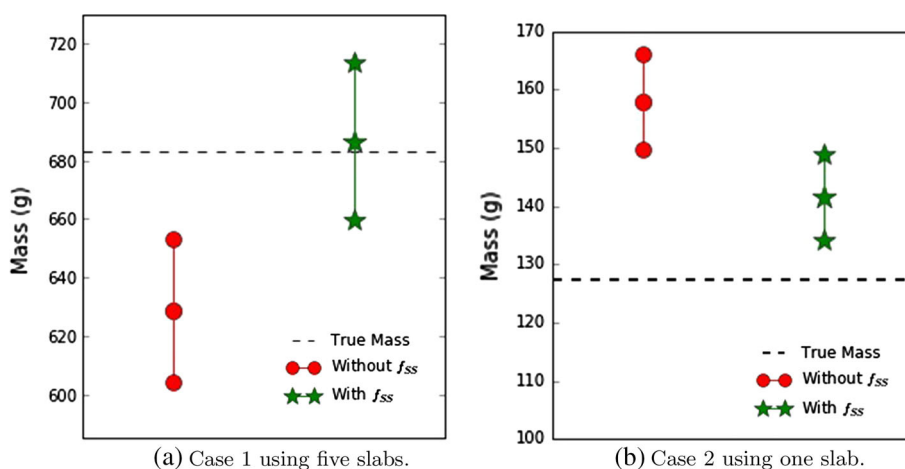


Figure 5. Mass determination with NAA measurements using the rectangular cuboid slabs as the unknown and three slabs as the comparator.

been accounted for within the scope of the current work. These factors lead to a large model error, resulting in the error between the true mass and approximated mass. Neutron self-shielding is another factor that was considered. However, it was out-ruled because it was noted that thicker sample cases, such as case 1 which had a thickness D three time that of case 1, had very good agreement with the actual measurement after the inclusion of the self-shielding factor.

The uncertainty of the approximated masses resulted from the stochastic uncertainty in the counts and the systematic uncertainty due to varying material composition between the sample and the comparator. This was

partly due to the short half-life of ^{28}Al . In the time it took to transport the sample from the neutron source to the detector and begin measurement, 40% to 50% of the source would decay away. Removing this delay alone could decrease the uncertainty by a factor of 2. The remaining sources of uncertainty are computational, from the self-shielding factor and geometric efficiency. As the uncertainty in counts decreases it is important to account for model error in the self-shielding factor and geometric efficiency calculation. This type of error would include incorrect dimensions in the MCNP6 model, non-uniform source distribution from the neutron activation and non-uniform sample composition.

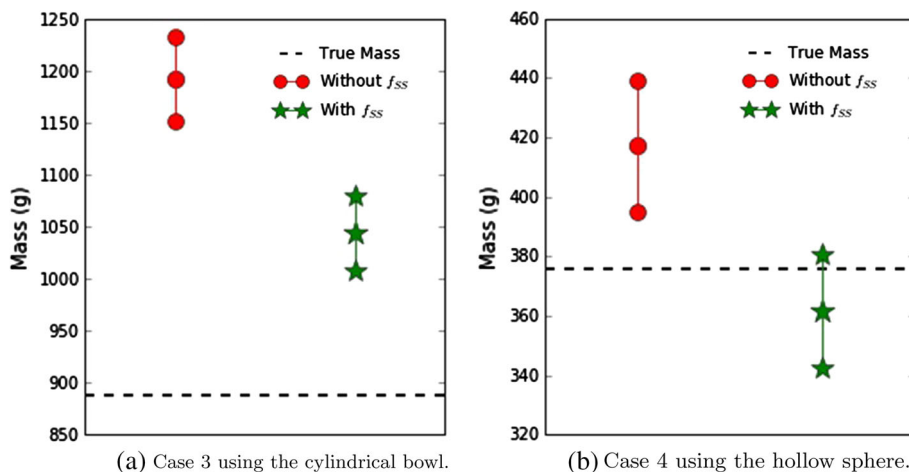


Figure 6. Mass determination with NAA measurements using cylindrical bowl and hollow sphere as the unknown and rectangular prism as the comparator.

Table 6. Calculated masses with and without self-shielding factor.

Case	Sample mass (g)	Comparator mass (g)	With f_{SS}			Without f_{SS}		
			m_{SS} (g)	$\sigma_{m_{SS}}$	$\Delta_{m_{SS}}$ (%)	m (g)	σ_m	Δ_m (%)
1	683.2	402.3	686.6	26.8	0.498	628.6	24.5	-7.992
2	127.5	402.3	143.0	7.4	12.16	159.5	8.3	25.10
3	888.3	683.2	1044.0	36.3	17.53	1191.8	41.5	34.17
4	376.0	683.2	361.7	19.0	-3.803	417.0	21.9	10.90

5. Conclusions

A method for improving non-destructive mass measurements using neutron activation analysis (NAA) by including the self-shielding factor for samples with a single element homogeneous composition but varying shapes was developed. By utilising MCNP6 simulations, as opposed to analytic methods, more complex geometries were modelled. Taking the magnitude of self-shielding into account, the mass of an unknown sample was experimentally determined by comparing it to the mass of a known sample using NAA and subsequent gamma spectroscopy. The experiments, performed at the Indian Institute of Technology-Kanpur, included the comparison of aluminum samples with various geometries and mass.

The inclusion of a self-shielding factor to this CMA has been shown to more accurately measure the mass of thick objects using NAA by reducing deviation from actual masses by a factor of 2 or more. Furthermore, CMA has been shown to work for heterogeneous geometries of a single element homogeneous composition by taking the self-shielding factor and geometric efficiency into account.

The next step in this work is to extend this work to samples comprising different materials and compositions, as motivated by the results of case 3 in this work. To do this, the production rate, the intrinsic detector efficiency and the branching ratios may no longer be assumed constant between samples of different composition because the photopeaks being compared are likely to be at different energies from varying radioisotopes. Therefore, there must be some method of measuring the detector efficiency. Furthermore, ways to decrease the uncertainty in the measurements need to be developed. Methods that extend the application to samples with mixed compositions will greatly broaden the usefulness of CMA.

Acknowledgements

The authors are thankful to the Department of Science and Technology India, Early Career Research Award ECR/2016/000471 for supporting this work and to the Research Abroad Program (a part of the Halliburton Engineering Global Programs, Texas A&M University).

References

- [1] G F Knoll, *Radiation Detection and Measurement*, 3rd edn (Wiley, Hoboken, 2000)
- [2] K A A Gamage and M J Joyce, *Appl. Radiat. Isotopes* **69**, 1521 (2011)
- [3] R D Evans and R O Evans, *Rev. Mod. Phys.* **20**, 305 (1948)
- [4] J P Francois, *Nucl. Instrum. Methods* **117**, 153 (1973)
- [5] D W Millsap and S Landsberger, *Appl. Radiat. Isotopes* **97**, 21 (2015)
- [6] M N Nasrabadi, A Mohammadi and M Jalali, *Appl. Radiat. Isotopes* **67**, 1208 (2009)
- [7] S Singh, *Mass determination using gamma-ray measurements*, Master's thesis (Indian Institute of Technology Kanpur, Uttar Pradesh, India, 2016)
- [8] S Prasad, N Pinchuk, S E Anderson and R F Fleming, *Nuclear Instrum. Methods Phys. Res. A* **624**, 180 (2010)
- [9] J L Parker, *Correction for gamma-ray self-attenuation in regular heterogeneous materials*, Technical Report LA-8987-MS (Los Alamos National Laboratory, 1981)
- [10] R A Purty and S Prasad, *Appl. Radiat. Isotopes* **125**, 144 (2017)
- [11] V F Sears, *Neutron News* **3**, 26 (1992)
- [12] M S Basunia, *Nucl. Data Sheets* **114**, 1189 (2013)
- [13] M J Berger, J H Hubbell, S M Seltzer, J Chang, R Sukumar, D S Zucker and K Olsen, XCOM: Photon Cross Section Database (version 1.5), <http://physics.nist.gov/xcom> (accessed on June 1st) (2016)
- [14] T Goorley *et al*, *Nucl. Technol.* **180**, 298 (2012)